GNSS multipath detection using three-frequency signal-to-noise measurements

Philip R R Strode and Paul D Groves

University College London

Abstract

A new technique for detecting GNSS multipath interference by comparing signal-to-noise (SNR) measurements on three frequencies is presented. Depending on the phase lag of the reflected signal with respect to the direct signal, multipath interference can be either constructive or destructive, with a commensurate effect on the measured SNR. However, as the phase lag is frequency-dependent, the SNR is perturbed differently on each frequency. Thus, by differencing SNR measurements on different frequencies and comparing the result with that obtained in a low-multipath environment, multipath can be detected. Using three frequencies makes the process more robust. A three-frequency SNR-based multipath detector has been developed and calibrated using measurements from GPS Block IIF satellites in a low-multipath environment. The new detector has been tested in a range of urban environments and its multipath-detection capability verified by showing that the MP observables oscillate when the new detection statistic is above a threshold value determined using data collected in a low-multipath environment. The new detector is also sensitive to diffraction.

Introduction

Global Navigation Satellite Systems (GNSS) 3D positioning has developed rapidly in the last 20 years, enabling real-time static and kinematic position at decimetre accuracies using differential techniques and centimetre accuracies using carrier phase techniques. This will continue to improve over the next 7 years as the GPS and GLONASS satellite constellations are joined by the increasing number of satellites in the European Galileo and Chinese Beidou systems. The majority of errors associated with GNSS positioning are effectively removed through modelling, filtering and differential technologies. However, multipath interference cannot be corrected in this way. There are many techniques for mitigating the effect of multipath interference on GNSS positioning; however, none of them are completely reliable. Thus, multipath interference remains a large source of error for real time applications, particularly in urban and offshore environments. We offer a unique approach to multipath detection and mitigation through new possibilities offered by GPS Block IIF and Galileo satellites transmitting on three frequencies. It builds on some preliminary work presented within Groves et al. (2013) and forms part of a wider programme of research to improve GNSS positioning

in dense urban areas (Jiang and Groves 2014; Groves and Jiang 2013; Wang et al. 2013; Hsu et al. 2014).

The proposed technique detects multipath interference by comparing measurements of carrier-power-to-noise-density ratio (C/N_0) on three frequencies. It works on the principle that multipath interference with a particular path delay will lead to constructive interference on some frequencies and destructive interference on others. Therefore, the difference in C/N_0 between frequencies will change in the presence of multipath interference. Once multipath has been detected, the affected signals may be either down-weighted in the position solution or excluded altogether. The new technique is most effective at detecting short-delay multipath interference, with sensitivity dropping as the path delay increases. Diffraction can also be detected, but not non-line-of-sight (NLOS) reception. Thus, this method is most suited to geodesy and surveying applications where short-delay multipath interference impedes precision carrier phase positioning and three-frequency receivers are commonly deployed.

We begin with a summary of the characteristics of multipath interference, NLOS reception and diffraction, followed by a brief review of current mitigation techniques. The new three-frequency multipath detection technique is then presented in detail and the calibration procedure described. Finally, test results from a number of static and kinematic environments around central London are presented and the impact of diffraction and NLOS reception assessed. A short discussion on mitigation using this technique completes the paper. All experimental data was collected using a Leica Viva GS15 geodetic GNSS receiver.

Characteristics of Multipath, NLOS and Diffraction

One of the most significant and hardest to mitigate error sources in GNSS positioning is multipath interference, where signals from a satellite are being received by the user through multiple paths. Multipath interference is often confused with NLOS and diffraction effects; however these are different phenomena that can act independently or simultaneously with multipath. An example of multipath interference is shown in Fig. 1.

Multipath interference is therefore of particular significance in areas such as urban canyon, city landscapes. However it is also important for large vessels and offshore structures due to the large body of the structure reflecting signals and also the water reflecting signals from low elevations. Reflections from large, smooth surfaces create specular multipath which causes a large error compared to diffuse multipath from coarse surfaces (Comp and Axelrad 1998). Each reflected signal has a certain amount of delay compared to the direct signal. This path delay arises because reflected signals follow a longer path. The strength of this delayed signal depends on the reflection coefficient of the reflective surface (Brodin and Daly 1997). Because the multipath interference depends on the

location of the receiver, it is not possible to eliminate the error by using differential techniques (Uren and Price 2010).

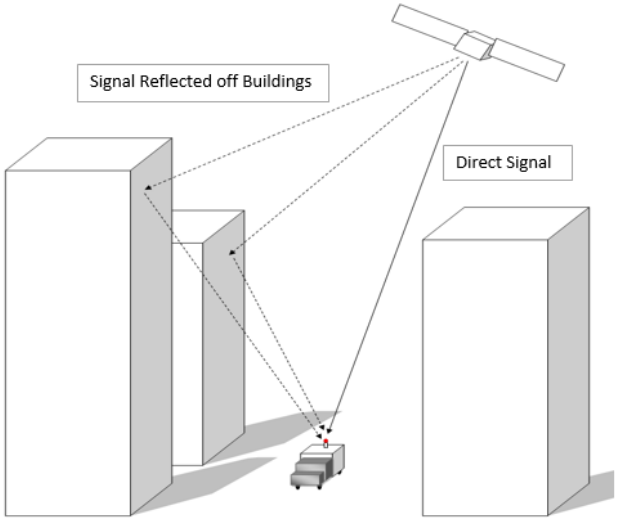

Fig. 1 Example of multipath interference

Multipath interference affects carrier phase and pseudorange measurements differently (Groves 2013; Brodin and Daly 1997). Pseudorange multipath is caused by the indirect signal interfering with the correlation of the pseudo random noise (PRN) code of the direct signal. This causes code tracking errors that depend on the signal and receiver designs as well as the properties of the reflected signal. The ranging error is largest where the path delay of the reflected signal is around half a code chip. The maximum error is proportional to the early-late correlator spacing, d, and the strength of the reflected signal. The ranging error is small for path delays that are very short or close to $(1 + d/2)$ code chips. If the path delay is greater than $(1 + d/2)$ code chips, the receiver will ignore the reflected signal completely. The ranging error also depends on the phase lag of the indirect signal with respect to the direct signal. If this is between –90° and +90°, constructive interference occurs and the ranging error is positive. Otherwise, the interference is destructive and the ranging error is negative. Phase lags of 0° and 180° maximize the interference and the resulting ranging error.

Carrier phase measurements are affected by multipath interference when the phase of the indirect signal is different from that of the direct signal. The error associated with carrier phase multipath is however limited to one quarter of the wavelength, assuming the reflected signal is no stronger than the direct signal. This is relatively small compared to the pseudorange multipath error.

Non-line-of-sight reception occurs when a signal is received via an indirect route from a given satellite that would otherwise have no line of sight to the user antenna due to buildings or other obstructions blocking the direct signal path. It is common in urban canyons. Signals may be reflected

from nearby or distant surfaces such as tall buildings. The range measurement error caused by NLOS reception is always positive and equal to the path delay, the difference between the reflected path taken by the received signal and the obstructed path from the satellite to the receiver (Groves 2013; Jiang and Groves 2014). NLOS reception therefore has the potential to cause limitless error. In practice, it ranges from a few metres, hundreds of metres or several kilometres if reflected via a distant building. This is an independent phenomenon to multipath interference; however the two occur simultaneously whenever the received signal is a combination of multiple reflected signals.

Alongside multipath interference and NLOS, signals can also be subject to diffraction from sharp edges of buildings and other obstacles within the signal path. When multiple diffractive sources are present, this causes the signal to interfere with itself and creates short-delay multipath even from buildings a long distance from the receiver. The effect is frequency-dependent and therefore the effects on the GPS L1, L2 and L5 signals will have varying scale and speed. Diffraction can also be combined with both multipath and NLOS. 3D models have been used to predict NLOS and diffracted signals (Bradbury 2007; Wang et al. 2012). However, for this paper, possible diffraction situations are determined simply by using the azimuth of the given satellite and the known position of obstructions from imagery mapping.

Current multipath mitigation techniques

Many different multipath and NLOS mitigation techniques have been developed in the past. Some have been implemented within commercial user equipment while others remain experimental. The main techniques may be organised into three categories: antenna-based, receiver-based and navigation-processor-based techniques.

Firstly, the antenna system may be designed to attenuate reflected signals. A change from right handed circularly polarized (RHCP) to left handed circularly polarized (LHCP) occurs when a GNSS signal is reflected specularly (assuming a smooth surface and an angle of incidence less than Brewster's angle). Therefore, the gain pattern of the antenna may be designed so that only RHCP are detected and LHCP signals are rejected (Granger and Simpson 2008). This works better with the larger higher-cost antennas used in professional receivers.

Similarly, a choke ring antenna can be deployed; this uses a ground plane around the bottom of the antenna to attenuate signals that have been reflected off the ground, together with concentric rings that are designed to attenuate low elevations signals, which are particularly vulnerable to reflection. However, this requires bulky equipment to be added to the user's antenna, so is not practical for many applications.

Receiver-based multipath mitigation techniques modify the design of the receiver in order to increase the resolution of the code discriminators, making it easier to distinguish the direct and reflected signals. Examples include the narrow correlator, double-delta and strobe correlator techniques. These techniques reduce the code tracking errors due to multipath interference with medium and large path delays. Vector tracking may also be used to reduce the impact of both multipath interference and NLOS reception on the position solution (Hsu et al. 2014).

Multipath interference and NLOS reception can also be mitigated within the navigation processor. Consistency checking takes advantage of the fact that the multipath-contaminated and NLOS signals will produce inconsistent position solutions and therefore by using only the consistent signals the position solution can be improved (Groves and Jiang 2013). 3D city models have also been used to predict NLOS signals for removal from the position solution (Obst et al. 2012; Peyraud et al. 2013).

There are many more multipath and NLOS mitigation techniques than there is room to discuss here. For a full review, readers are directed to Groves et al. (2013) for techniques suitable for real-time implementation, Buiyan and Lohan (2012) for receiver-based techniques, and Lau and Cross (2007) for techniques suited to high-precision post-processed applications. Each mitigation technique reduces the impact of multipath interference and/or NLOS reception. However, none of them eliminate the problem completely. Therefore, there is still a need for additional techniques.

Multipath Detection by Signal-to-noise ratio

GNSS receivers output signal-to-noise ratio, SNR, measurements for each satellite tracked in dB-Hz. The SNR measurement is usually an approximation of the carrier-power-to-noise-density, C/N_0, the ratio of the received signal power, P, to the weighted noise power spectral density, N_0. With a good antenna in an interference-free environment, the SNR should be over 42 dB-Hz (Groves 2013; Ward et al. 2006; Bilich et al. 2007).

In the presence of multipath interference, the absolute (i.e. non-decibel) SNR is proportional to $A_d^2 + A_m^2 + 2A_dA_m\cos\varphi$, where A_d is the amplitude of the direct signal, A_m is the amplitude of the reflected signal after code correlation, and φ is the relative phase difference between the reflected and direct signal (Bilich et al. 2007). Constructive multipath interference causes the SNR to increase while destructive interference causes it to decrease. The SNR thus oscillates over time as the phase lag of the reflected signal varies. The amplitude of the oscillation depends on the path delay as well as the amplitudes of the direct and reflected signals and is larger for short-delay multipath. This is because the SNR is typically measured using the prompt correlator outputs, which are affected more by the

reflected signal when the path delay is short. The carrier phase ranging error also oscillates with the same period as the SNR, but is 90° out of phase.

A number of techniques for multipath detection and correction based on the oscillation of the SNR measurements over time have been developed (Comp and Axelrad 1996; Lau and Cross 2007; Rost and Wanninger 2009). One technique, known as power spectral mapping, uses the SNR measurements to map the multipath environment, giving an image of the reflective objects that have sent indirect signals to the receiver (Bilich and Larson 2008; Benton and Mitchell 2011). However, all of these techniques require post-processing of the data. Here, we investigate the use of SNR measurements for multipath detection in real time.

The problem with trying to identify multipath interference from instantaneous SNR measurements is that multipath is one of many reasons why the SNR may depart from normal. Other causes include signal attenuation by buildings, people, vehicles and foliage; interference, including jamming; satellite power variation; NLOS reception and diffraction. However, attenuation has similar effects on all signals from a given satellite, while interference and jamming have similar effects on signals from different satellites on the same frequency. It is only the effects on SNR of multipath interference and diffraction that depend on both the satellite and the frequency. Constructive and destructive interference happens at different times on different frequencies because the relative phase difference, φ, between the reflected and direct signal for a given path delay depends on the wavelength of the signal as illustrated in Fig. 2. Therefore, there is potential to rapidly detect multipath interference by comparing SNR measurements made on different frequencies.

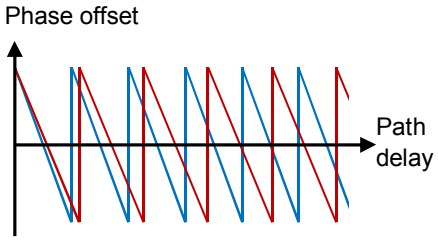

Fig. 2 Phase offset of the reflected signal with respect to the direct signal on two different frequencies (shown in red and blue, respectively) as a function of the path delay

Preliminary experiments to test this idea are described in Rudi (2012) and Groves et al. (2013). Multi-frequency GPS and GLONASS data was collected in both low-multipath and high-multipath environments. Measured SNR differences between the L1 and L2 frequencies and, where available between L1 and L5, were plotted against elevation and the low- and high-multipath data compared. At a given elevation, the inter-frequency SNR differences in the low-multipath environment comprised a constant plus noise.

In the high-multipath environment, large oscillations in both the L1–L2 and L1–L5 SNR differences were observed at certain times for certain satellites. To determine whether this might be due to multipath interference, the MP1 observable was calculated. The MP1, MP2 and MP51 observables given by (Hilla and Cline 2004):

$$\begin{aligned} MP1_a^s &= \widetilde{\rho}_{a,S}^{s,\mathrm{L1}} - \left(\frac{\left(f_{ca}^{\mathrm{L1}}\right)^2 + \left(f_{ca}^{\mathrm{L2}}\right)^2}{\left(f_{ca}^{\mathrm{L1}}\right)^2 - \left(f_{ca}^{\mathrm{L2}}\right)^2} \right) \widetilde{\Phi}_{a,R}^{s,\mathrm{L1}} + \frac{2\left(f_{ca}^{\mathrm{L2}}\right)^2}{\left(f_{ca}^{\mathrm{L1}}\right)^2 - \left(f_{ca}^{\mathrm{L2}}\right)^2} \widetilde{\Phi}_{a,R}^{s,\mathrm{L2}} \\ MP2_a^s &= \widetilde{\rho}_{a,S}^{s,\mathrm{L2}} - \frac{2\left(f_{ca}^{\mathrm{L1}}\right)^2}{\left(f_{ca}^{\mathrm{L1}}\right)^2 - \left(f_{ca}^{\mathrm{L2}}\right)^2} \widetilde{\Phi}_{a,R}^{s,\mathrm{L1}} + \left(\frac{\left(f_{ca}^{\mathrm{L1}}\right)^2 + \left(f_{ca}^{\mathrm{L2}}\right)^2}{\left(f_{ca}^{\mathrm{L1}}\right)^2 - \left(f_{ca}^{\mathrm{L2}}\right)^2} \right) \widetilde{\Phi}_{a,R}^{s,\mathrm{L2}} \\ MP51_a^s &= \widetilde{\rho}_{a,S}^{s,\mathrm{L5}} - \frac{2\left(f_{ca}^{\mathrm{L1}}\right)^2}{\left(f_{ca}^{\mathrm{L1}}\right)^2 - \left(f_{ca}^{\mathrm{L5}}\right)^2} \widetilde{\Phi}_{a,R}^{s,\mathrm{L1}} + \left(\frac{\left(f_{ca}^{\mathrm{L1}}\right)^2 + \left(f_{ca}^{\mathrm{L5}}\right)^2}{\left(f_{ca}^{\mathrm{L1}}\right)^2 - \left(f_{ca}^{\mathrm{L5}}\right)^2} \right) \widetilde{\Phi}_{a,R}^{s,\mathrm{L5}} \end{aligned} \tag{1}$$

where $\widetilde{\rho}_{a,S}^{s,l}$ is the pseudorange measurement from satellite s to user antenna a on frequency l, $\widetilde{\Phi}_{a,R}^{s,l}$ is the corresponding accumulated delta range (ADR), derived from carrier phase measurements, and f_{ca}^{l} is the carrier frequency. For GPS, $l \in$ L1, L2, L5. The change over time in the true pseudorange, troposphere and ionosphere propagation delays largely cancel out, leaving a parameter dominated by the L1 code multipath error and tracking noise. It was found that the oscillations in the SNR differences coincided with oscillations in the MP1 parameter, confirming the multipath hypothesis. The amplitudes of the oscillations did not correspond because the MP1 amplitude is proportional to that of the code multipath error, whereas the SNR difference amplitude is proportional to that of the carrier phase multipath error.

It can thus be concluded from the preliminary experiments that strong multipath could be detected by comparing the measured inter-frequency SNR difference with its expected value in a low-multipath environment at the same elevation. However, a fundamental limitation of this approach is that, for certain reflected signal path delays, the phase lag is approximately the same on both frequencies with the result that the SNR difference is not always perturbed when multipath is present. Consequently, the technique may only work half the time. More reliable detection can be achieved by using three frequencies as the phase of the multipath interference is much less likely to be consistent across three frequencies than across two. Three-frequency SNR-based multipath detection thus forms the main subject.

Proposed Three-Frequency SNR-Based Multipath Detector

In general terms, a fault detection algorithm computes a test statistic from a set of current measurements and then compares it with a threshold that marks the limit of the system's normal performance. If the test statistic exceeds the threshold, a fault is deemed to be present. For GNSS multipath detection, the aim is to both compare the SNR measurement on each frequency with its

expected value under good reception conditions and to eliminate effects common to all frequencies. The following detection statistic meets these requirements:

$$S_a^s = \sqrt{\begin{aligned}&\left[\left(\widetilde{C}/\widetilde{N}_0\right)_a^{s,\mathrm{L1}} - \left(\widetilde{C}/\widetilde{N}_0\right)_a^{s,\mathrm{L2}} - \Delta C^{12}\left(\theta_{nu}^{as}\right)\right]^2 \\ &+\left[\left(\widetilde{C}/\widetilde{N}_0\right)_a^{s,\mathrm{L1}} - \left(\widetilde{C}/\widetilde{N}_0\right)_a^{s,\mathrm{L5}} - \Delta C^{15}\left(\theta_{nu}^{as}\right)\right]^2\end{aligned}} \tag{2}$$

where $\left(\widetilde{C}/\widetilde{N}_0\right)_a^{s,l}$ is the measured C/N_0 (in dB-Hz) by receiver a of signal l from satellite s; ΔC^{12} and ΔC^{15} are, respectively, the predicted L1–L2 and L1–L5 C/N_0 differences assuming a low-multipath environment; and θ_{nu}^{as} is the elevation angle of satellite s from user antenna a. Strong multipath interference is assumed present whenever the test statistic exceeds a threshold, T. The predicted L1–L2 and L1–L5 C/N_0 differences and the test threshold are modeled as a function of elevation because the user-antenna gain varies with elevation. The remainder describes the calibration and testing of this detector.

It is assumed that a receiver's SNR measurement approximates C/N_0. Thus, the SNR measurements output by the Leica Viva GS15 geodetic GNSS receiver used in our experiments is the source of all of the C/N_0 data.

The multipath detector was calibrated using 14 hours of data collected in a low-multipath environment. The selected site, shown in Fig. 3, was on a small hill on a golf course at Felixstowe, Suffolk, UK. Data at elevations of 10° and above from satellites PRN 24, 25 and 27 was used in the subsequent analysis; these were the only satellites transmitting the GPS L5 signal that were receivable at a convenient time.

Fig. 3 Reference data acquisition in a low multipath environment at Felixstowe

Functions for the predicted L1–L2 and L1–L5 C/N_0 differences, ΔC^{12} and ΔC^{15}, as a function of elevation were obtained by fitting third-order polynomials to the corresponding low-multipath calibration data. The following were obtained:

$$\begin{aligned}\Delta C^{12}\left(\theta_{nu}^{as}\right) &= 2+0.098\theta_{nu}^{as}-0.0011\left(\theta_{nu}^{as}\right)^2+2.8\times10^{-6}\left(\theta_{nu}^{as}\right)^3 \text{ dB-Hz}\\ \Delta C^{15}\left(\theta_{nu}^{as}\right) &= -2.9+0.16\theta_{nu}^{as}-0.0016\left(\theta_{nu}^{as}\right)^2+4.7\times10^{-6}\left(\theta_{nu}^{as}\right)^3 \text{ dB-Hz}\end{aligned} \tag{3}$$

where the elevation angle, θ_{nu}^{as}, is in degrees. The polynomial functions and source data are shown in Fig. 4. The standard deviations of the L1–L2 and L1–L5 residuals are 1.11 dB-Hz and 0.98 dB-Hz, respectively, noting that the residuals are larger for elevations below 25°. These values are antenna- and receiver-dependent so will vary according to the equipment used. It may also be necessary to use different values for different GNSS signal designs.

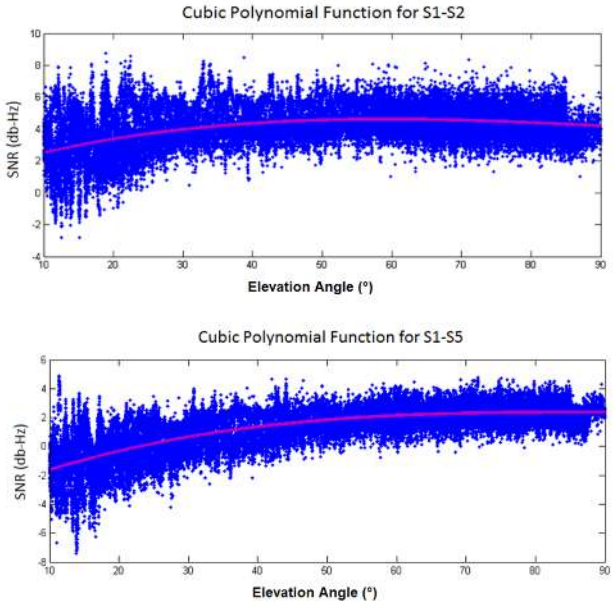

Fig. 4 Predicted L1–L2 and L1–L5 C/N0 differences (red) and their source data (blue)

To determine the detection threshold, the detection statistic, S_a^s, was computed for all of the low-multipath calibration data. A mean value, expressed as a function of elevation, was then computed by fitting a third-order polynomial. Finally, a single-value standard deviation across all elevations was computed; this was 0.88 dB-Hz. From these, three trial detection thresholds were computed, comprising mean plus standard deviation, T_σ, mean plus two standard deviations, $T_{2\sigma}$, and mean plus three standard deviations, $T_{3\sigma}$. The thresholds as a function of elevation are given by

$$\begin{aligned}T_{\sigma}\left(\theta_{nu}^{as}\right) &= 3.8795-0.082\theta_{nu}^{as}+0.0012\left(\theta_{nu}^{as}\right)^2-5.9\times10^{-6}\left(\theta_{nu}^{as}\right)^3 \text{ dB-Hz}\\ T_{2\sigma}\left(\theta_{nu}^{as}\right) &= 4.7589-0.082\theta_{nu}^{as}+0.0012\left(\theta_{nu}^{as}\right)^2-5.9\times10^{-6}\left(\theta_{nu}^{as}\right)^3 \text{ dB-Hz}\\ T_{3\sigma}\left(\theta_{nu}^{as}\right) &= 5.6384-0.082\theta_{nu}^{as}+0.0012\left(\theta_{nu}^{as}\right)^2-5.9\times10^{-6}\left(\theta_{nu}^{as}\right)^3 \text{ dB-Hz}\end{aligned} \tag{4}$$

where the elevation angle, θ_{nu}^{as}, is in degrees. These values are also antenna- and receiver-dependent. Fig. 5 shows the satellite PRN27 test statistic from the low-multipath calibration data, together with the three thresholds. This has a standard deviation of 1.18 dB-Hz, which is larger than that of the reference data as a whole. To minimize the false alarm rate, the 3 standard deviation threshold has been selected for multipath detection.

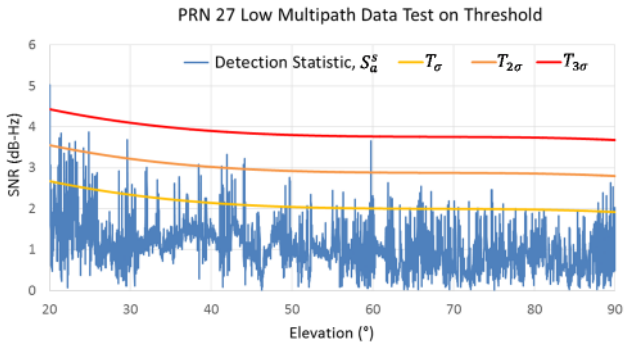

Fig. 5 Multipath detection statistic and thresholds in low-multipath environment

Multipath Detection Performance - Static

Three locations in Central London were chosen to carry out multipath observations of several hours with which to test the proposed multipath detection technique. These locations were chosen for their unique environments that would offer different multipath interference effects. The first location was located at Birkbeck College, Torrington Square. This was chosen as the glass building of Birkbeck offers large surfaces that are smooth relative to GNSS wavelengths and these typically act as strong specular reflectors (Ward et al 2006). The GNSS receiver was positioned 10m from the reflective surface (Fig. 6) and was logging data for 2 hours. As the data acquisition took place in the afternoon, the best elevation and visibility was offered by PRN 25. For this first test, the location of the receiver meant that there was a clear line of sight to the satellite at all times and no diffraction or NLOS could interfere with the signal. This enabled a multipath test to be carried out independently of the other phenomena. The multipath detection statistic and three standard deviation percentile threshold are presented as a time series in Fig. 7 along with the MP1 and MP51 observables for comparison. Note that all pseudorange measurements output by Leica receivers are carrier-smoothed, so the MP observables are commensurately reduced.

Fig. 6 Birkbeck College, Torrington Square multipath environment

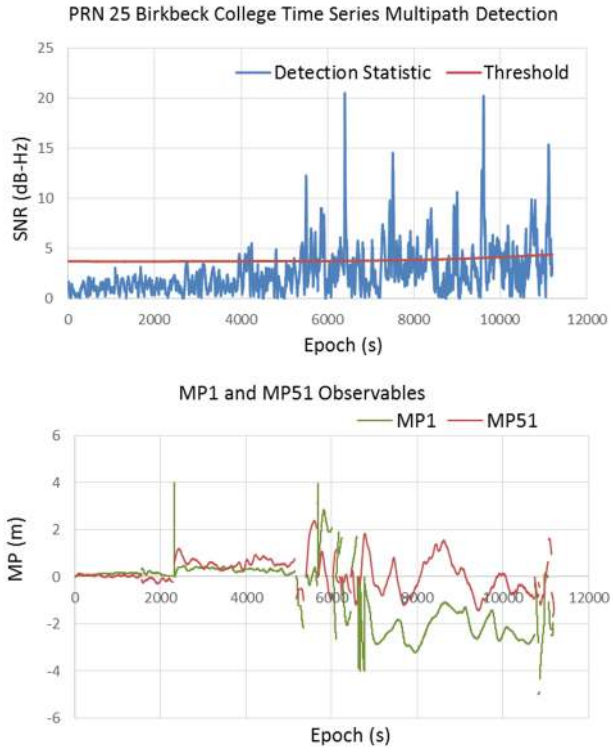

Fig. 7 PRN 25 Birkbeck College multipath environment observation results

Over the first 4000s, there is little variation in the MP observables and thus little multipath interference. This is due to the high elevation of the satellite. Later, the satellite is descending to lower elevations, resulting in large oscillations in the MP observables during the remainder of the observation period, which may be attributed to multipath interference. There is a strong correlation between the majority of peaks in the SNR-based detection statistic and the large variations in the MP observables. Discontinuities in the MP observables occur when the receiver resets. There is a large MP spike around 2300s which is not reflected in the detection statistic; this could be due to the SNR-

based detection being more sensitive to short-delay multipath and the MP observables being more sensitive to medium-delay multipath. However, the majority of the multipath interference is likely to be caused by a reflective surface roughly 10m from the receiver and will therefore be short-delay.

The second location, shown in Fig. 8, was the UCL Print Room Café, located on the Bloomsbury campus. Here, the receiver was placed very close (<1m) to the glass surface of the building. The location is enclosed with nearby buildings so will be able to offer a variety of multipath, diffraction and NLOS interference. Satellites were tracked during the hours around midday and therefore PRN 24 and 25 were tracked for their strong elevation and visibility.

Fig. 8 UCL Print Room Cafe high multipath environment

The detection statistic and the three standard deviation threshold for PRN 25 are compared with the MP observables in Fig. 9. Note that tracking is interrupted around 3000s and between 6500s and 8000s. After 4600s, the receiver resets every 70s or so, producing discontinuities in the MP observables. This clearly demonstrates that this is a challenging environment. However, it is difficult to determine from the MP observables when multipath is present. The new SNR-based detector frequently detects multipath. Note that there is a brief period of stability around 9200s, during which the MP observables are stable and the SNR-based detection statistic is well below the threshold.

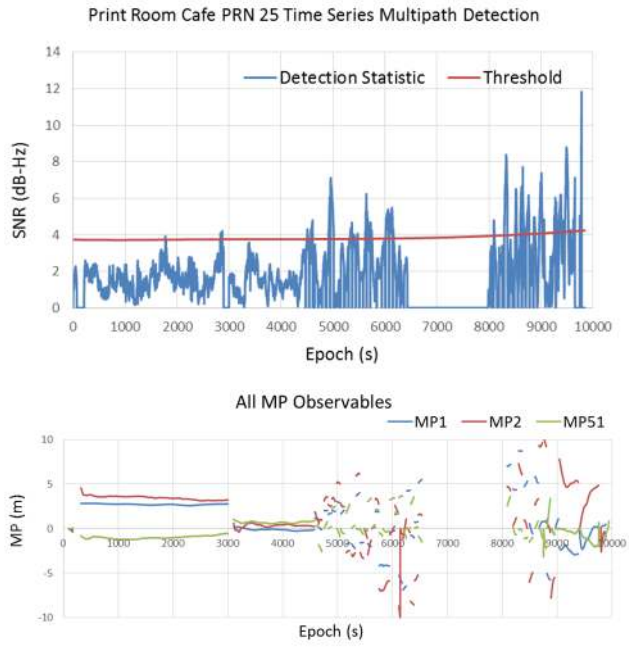

Fig. 9 PRN 25 UCL Print Room Cafe multipath environment observation results

The third multipath environment, shown in Fig. 10, was Regent's Place in central London. This is a commercial area which incorporates a square surrounded by high rise buildings. This environment is ideal for a variety of multipath, diffraction and NLOS interference cases. It is particularly good for analysing diffraction effects as the satellite signals are lost and then re-emerge from behind the buildings.

Fig. 10 Regent's Place multipath environment

Again, PRN 25 provides the longest dataset. The results of this observation period are presented in Fig. 11, showing the detection statistic, MP observables and absolute SNR values. Where

there was loss of lock on any one frequency, the SNR-base detection statistic was set to zero to avoid large spikes.

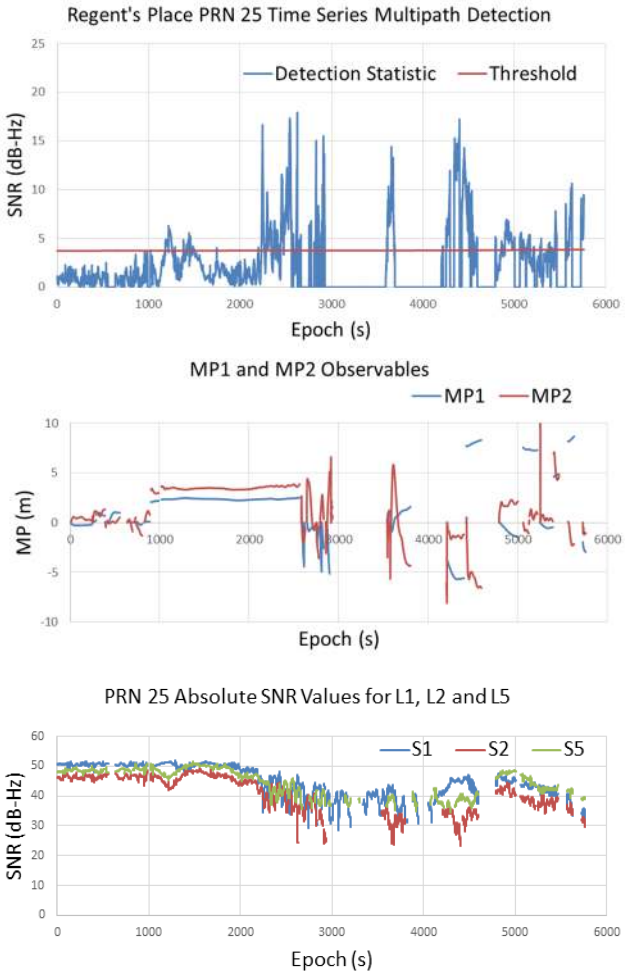

Fig. 11 Regent's Place PRN 25 multipath environment observation results

Over the first 800s, the SNR-based detection statistic is stable, but the effects of receiver resets can be seen. This could be due to problems with other signals. Around 800-1000s, slight fluctuation in the MP observables that is seen, during which, the SNR-based detection statistic is just below the detection threshold. However, between 1200 and 1500s and again between 2200 and 2600s, multipath is detected by the SNR-based detection statistic. However, the MP observables are stable, not showing any signs of multipath interference at all. The absolute SNR values, presented in Fig. 11, show that the signal is attenuated at both these times. This is likely to be diffraction as the proposed detection statistic is sensitive to this, whereas the MP observables are not. From 2600s until tracking is lost on L2 at around 2900s, the MP observables show significant oscillation. This is due to the fact

that once the signal is diffracted and behind the building, the receiver picked up NLOS signals. The SNRs oscillate steadily if there are multiple reflected paths but remain attenuated.

The diffraction hypothesis is confirmed by comparing the azimuth of satellite PRN 25, shown in Fig. 12, with that of the building edge, shown in Fig. 13. At 2091s, the satellite azimuth reaches about 80°, at which point, diffraction can be expected to start. The azimuth reaches 85° at 2646s; beyond this, the direct signal can be assumed completely blocked. At this point the elevation of the satellite is 65.6°, whereas the building masks elevations up to about 75°.

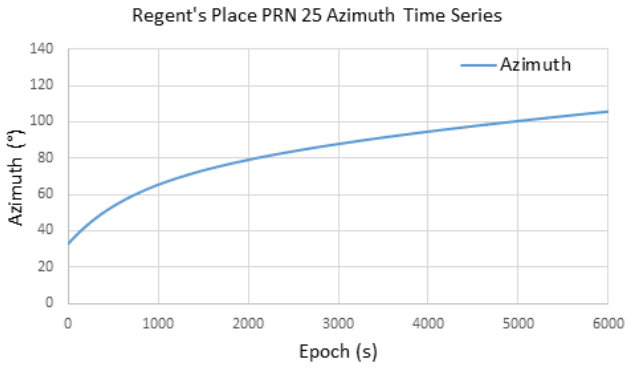

Fig. 12 PRN 25 azimuth time series at Regent's Place

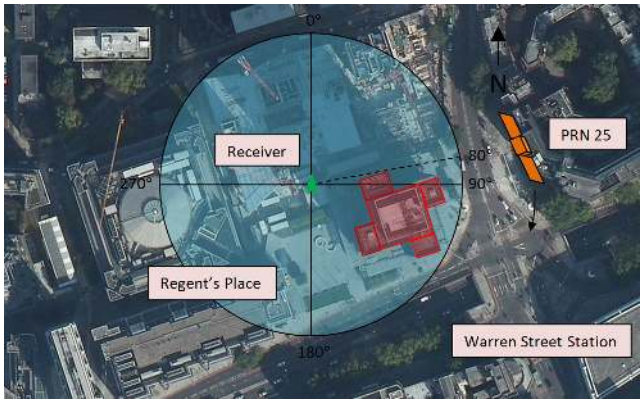

Fig. 13 Regent's Place location with building azimuth (image from Bing Maps, 2013)

After 4200s, the detection statistic is spiking frequently, whilst the MP observables are unstable. The results of this experiment show that the proposed SNR-based technique is successful at detecting short-delay multipath interference and diffraction. It also detects reception via multiple reflected paths when the direct signal is blocked, which is the simultaneous occurrence of NLOS reception and multipath interference.

Multipath Detection Performance - Kinematic

Many GNSS applications require a real-time dynamic positioning solution. Therefore, the proposed multipath detection technique was also test using kinematic observations. For these, the receiver was mounted on a pole whilst the user walked certain routes around UCL's Bloomsbury Campus in London. The routes were planned to incorporate a variety of high- and low-multipath environments as well as areas that may cause diffraction and NLOS reception. Both routes were of 30 minutes duration and are shown in Fig. 14. These tests were timed such that satellite PRN 25 was at high elevation (descending from 83° to 76°) for route 1 and mid elevation (descending from 56° to 47°) for route 2.

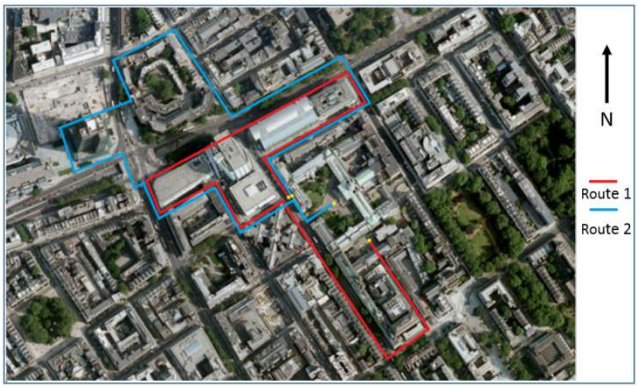

Fig. 14 Routes 1 and 2 around UCL Bloomsbury campus (image from Google Maps, 2013)

The detection statistic and MP51 observable for satellite PRN 25 from route 1 are shown in Fig. 15. Multipath interference was detected using the new technique at 300-350s, 440-460s, 900-950s and around 1200s. These are confirmed by the MP51 observable, noting that the magnitudes don't match because the SNR-based technique is more sensitivity to short-delay multipath and the MP51 observable to medium-delay. Discontinuities in the MP51 observable can be seen following periods when tracking lock is lost or the receiver resets can clearly be seen, noting that the SNR-based detection statistic is set to zero when lock is lost on one or more frequency.

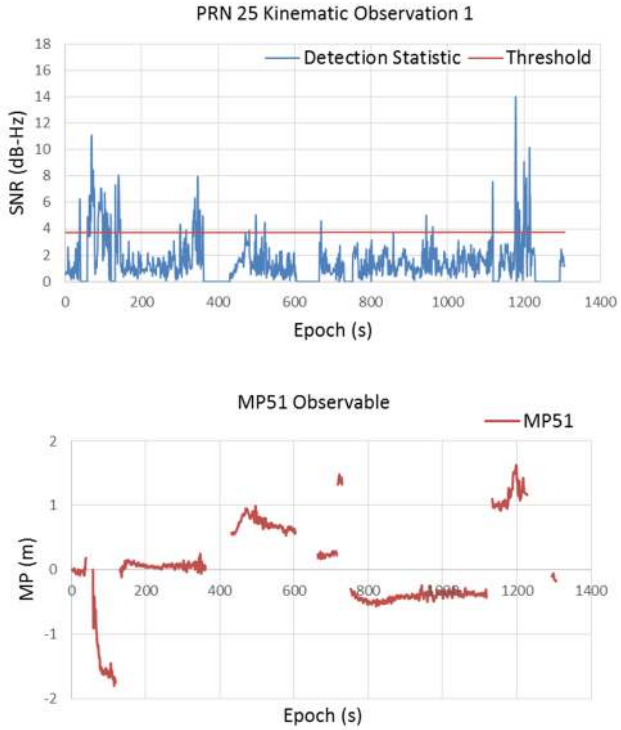

Fig. 15 PRN 25 Kinematic observation 1 results

One noticeable feature in the results is the large increase in the detection statistic from between 50 and 150s. At the same time, there is a large change in the MP observables. Examination of the absolute SNR values in Fig. 16 shows that the signal is attenuated, indicating NLOS reception. NLOS reception accounts for the behaviour of the MP observables. The peaks in the SNR-based detection statistic are likely to be caused by reception of multiple reflected signals.

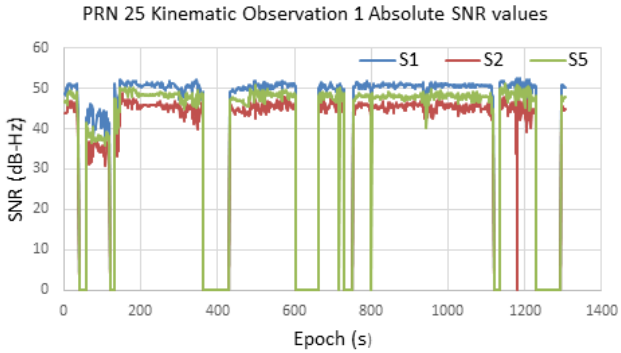

Fig. 16 PRN 25 Kinematic observation 1 absolute SNR values

The results for route 2, where PRN 25 was at a lower elevation, can be seen in Fig. 17. Here, there were significant periods of loss of lock which are reflected in both the detection statistic (zero values) and the MP observable (spikes). However, around 300s, between 800 and 1000s and between 1200 and 1400s, the SNR-based detection statistic is successfully indicating multipath. The majority of the peaks in the detection statistic correlate with the MP observable.

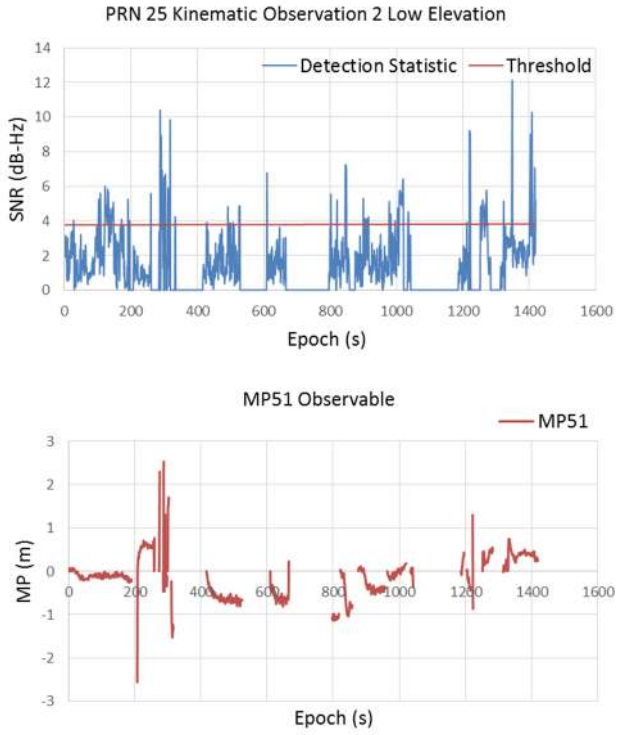

Fig. 17 PRN 25 Kinematic observation 2 results

From Detection to Mitigation

The focus here is on multipath detection. However, once multipath has been detected, its effects should be mitigated. The affected signals may be either down-weighted in the position solution or excluded altogether. Which approach is best depends on both the quality of the available signals from other satellites and the severity of the multipath. One approach is to set two detection thresholds with signals detected by the upper threshold removed completely from a position solution, while those detected only by the lower threshold are down-weighted. Finally, this new detection technique should be used to augment outlier detection, not replace it. Neither technique is completely reliable, so a combined approach can be expected to work better than either technique on its own. All of these issues are subjects for future research.

Conclusions

A new multipath detection technique has been developed, based on measuring discrepancies between the signal-to-noise ratios on different frequencies that occur during multipath interference. Three frequencies are used for better reliability. The detection statistic and threshold have been calibrated using data collected in a low-multipath environment. The new detection technique has been tested both statically and kinematically in a range of urban environments using a geodetic receiver. Its capability to detect both multipath interference and diffraction has been verified. It is recommended that the technique is deployed as part of a portfolio of multipath and NLOS mitigation techniques (Groves et al. 2013).

Acknowledgements

The authors thank Aled Jones and Cyrus Mills for their help during the data capture phase, and Dr Ziyi Jiang for his technical advice and support with the data processing software.

References

Benton C, Mitchell C (2011) Isolating the Multipath Component in GNSS Signal-to-Noise Data and Locating Reflecting Objects. Radio Science 46(6): RS6002

Bhuiyan MZH, Lohan ES (2012) Multipath Mitigation Techniques for Satellite-Based Positioning Applications. in Jin S (Ed.) Global Navigation Satellite Systems: Signal, Theory and Applications, InTech, Rijeka, Croatia, 405-426

Bilich A, Axelrad P, Larson K (2007) Scientific Utility of the Signal-to-Noise Ratio (SNR) Reported by Geodetic GPS Receivers. Proc. ION GNSS 2007, Institute of Navigation, Fort Worth, TX, September, 1999-2010

Bilich A, Larson K (2008) Mapping the GPS Multipath Environment Using the Signal-to-Noise Ratio (SNR). Radio Science 42(6): RS6003

Bradbury J (2007) Prediction of Urban GNSS Availability and Signal Degradation Using Virtual Reality City Models. Proc. ION GNSS 2007, Institute of Navigation, Fort Worth, TX, September, 2696-2706

Brodin G, Daly P (1997) GNSS Code and Carrier Tracking in the Presence of Multipath. International Journal of Satellite Communications 15(1):25-34

Comp CJ, Axelrad P (1996) An Adaptive SNR-based Carrier Phase Multipath Mitigation Technique. Proc. ION GPS-96, Institute of Navigation, Kansas City, MO, September, 683-697

Comp CJ, Axelrad P (1998) Adaptive SNR based carrier phase multipath mitigation technique. IEEE Transactions on Aerospace and Electronic Systems 34(1):264-276

Granger R, Simpson S (2008) An Analysis of Multipath Mitigation Techniques suitable for Geodetic Antennas. Proc. ION GNSS 2008, Institute of Navigation, Savannah, GA, September, 2755-2765

Groves PD (2013) Principles of GNSS, Inertial, and Multisensor Navigation Systems, 2nd edn. Artech House, Boston

Groves PD et al. (2010) Novel Multipath Mitigation Methods using a Dual-polarization Antenna. Proc. ION GNSS 2010, Institute of Navigation, Portland, OR, September, 140-141

Groves PD, Jiang Z (2013) Height Aiding, C/N_0 Weighting and Consistency Checking for GNSS NLOS and Multipath Mitigation in Urban Areas. Journal of Navigation, 66(5):653-659. doi: 10.1017/S0373463313000350

Groves PD, Jiang Z, Wang L, Ziebart MK (2012) Intelligent Urban Positioning Using Multi-Constellation GNSS with 3D Mapping and NLOS Detection. Proc. ION GNSS 2012, Institute of Navigation, Nashville, TN, September, 458-472

Groves PD, Jiang Z, Rudi M, Strode P (2013) A Portfolio Approach to NLOS and Multipath Mitigation in Dense Urban Areas, Proc. ION GNSS+ 2013, Institute of Navigation, Nashville, TN, September, 3231-3247

Hilla S, Cline M (2004) Evaluating pseudorange multipath effects at stations in the National CORS network. GPS Solutions 7(4):253-267

Hsu L-T, Jan S-S, Groves PD, Kubo N (2014) Multipath mitigation and NLOS detection using vector tracking in urban environments. GPS Solutions doi: 10.1007/s10291-014-0384-6

Jiang Z, Groves PD (2014) NLOS GPS signal detection using a dual-polarisation antenna. GPS Solutions 18(1):15-26. doi: 10.1007/s10291-012-0305-5

Lau L, Cross P (2007) Investigations into Phase Multipath Mitigation Techniques for High Precision Positioning in Difficult Environments. Journal of Navigation 60(3): 95-105

Obst M, Bauer S, Wanielik G (2012) Urban Multipath Detection and mitigation with Dynamic 3D Maps for Reliable Land Vehicle Localization. Proc. IEEE/ION Position, Location, and Navigation Symposium 2012, Myrtle Beach, SC, April, 685-691

Peyraud S et al. (2013) About Non-Line-Of-Sight Satellite Detection and Exclusion in a 3D Map-Aided Localization Algorithm. Sensors 13(1): 829-847

Rost C, Wanninger L (2009) Carrier Phase Multipath Mitigation Based on GNSS Signal Quality Measurements. Journal of Applied Geodesy 3(2):81-87

Rudi M (2012) GNSS Multipath Detection and Mitigation from Multiple-Frequency Measurements, MSc Dissertation, University College London

Uren J, Price B (2010) Surveying for Engineers, 5th edn. Palgrave Macmillan, Basingstoke

Wang L, Groves PD, Ziebart MK (2012) Multi-Constellation GNSS Performance Evaluation For Urban Canyons Using Large Virtual Reality City Models. Journal of Navigation 65(2):459-476

Wang L, Groves PD, Ziebart MK (2013) GNSS Shadow Matching: Improving Urban Positioning Accuracy Using a 3D City Model with Optimized Visibility Scoring Scheme. NAVIGATION, 60(3):195-207

Ward PW, Betz JW, Hegarty CJ (2006) Interference, Multipath, and Scintillation. in Kaplan E, Hegarty CJ (eds) Understanding GPS Principles and Applications, 2nd edn. Artech House, Boston, 243-299

Philip R. R. Strode completed an MSc in Hydrographic Surveying at University College London (UCL) in 2013, receiving a distinction. He holds a BA in Archaeology from the University of Nottingham and now works as an offshore surveyor with Fugro, where his responsibilities include the setup, testing, calibration and operation of a variety of survey and positioning systems.

Paul D. Groves is a Lecturer (academic faculty member) at UCL, where he leads a program of research into robust positioning and navigation. He joined in 2009, after 12 years at DERA and QinetiQ. He is interested in all aspects of navigation and positioning, including multi-sensor integrated navigation, improving GNSS performance under challenging reception conditions, and novel positioning techniques. He is an author of more than 70 technical publications, including the book Principles of GNSS, Inertial and Multi-Sensor Integrated Navigation Systems, now in its second edition. He is a Fellow of the Royal Institute of Navigation and holds a bachelor's degree and doctorate in physics from the University of Oxford.